

Determining the internal quantum efficiency of highly efficient polymer solar cells through optical modeling

L. H. Slooff, S. C. Veenstra,^{a)} and J. M. Kroon

Energy Research Centre of the Netherlands (ECN), P.O. Box 1, 1755 ZG Petten, The Netherlands and Dutch Polymer Institute, Eindhoven NL-5600 AX, The Netherlands

D. J. D. Moet

Zernike Institute for Advanced Materials, University of Groningen, Nijenborgh 4, 9747 AG Groningen, The Netherlands and Energy Research Centre of the Netherlands (ECN), P.O. Box 1, 1755 ZG Petten, The Netherlands

J. Sweelssen and M. M. Koetse

Holst Centre/TNO, Hightech Campus 48, Eindhoven 5656 AE, The Netherlands and Dutch Polymer Institute, Eindhoven NL-5600 AX, The Netherlands

(Received 25 January 2007; accepted 23 February 2007; published online 3 April 2007)

A power conversion efficiency of 4.2% (AM1.5, 1000 W/m²) is measured for an organic solar cell based on an active layer of an alternating copolymer, containing a fluorene and a benzothiadiazole unit with two neighboring thiophene rings, and a fullerene derivative. Using optical modeling, the absorption profile in the active layer of the solar cell is calculated and used to calculate the maximum short circuit current. The calculated currents are compared with measured currents from current-voltage measurements for various film thicknesses. From this the internal quantum efficiency is estimated to be 75% at the maximum for the best device. © 2007 American Institute of Physics. [DOI: 10.1063/1.2718488]

Since the discovery of electrical conductivity in doped polyacetylene in 1977,¹ much attention has been drawn to conjugated polymers. It was realized that this class of organic materials offers advantageous properties as compared to inorganic semiconductors, such as their mechanical flexibility, the tunability of their optoelectronic properties, easy incorporation in various kinds of devices, and above all, low-cost fabrication of these devices.² The high potential of conjugated polymers in solar cell applications has already become visible in polymer:fullerene bulk heterojunction solar cells with power conversion efficiencies (PCEs) approaching 5%.³

In recent years, polyfluorenes have gathered much attention in organic light emitting diode research, because of their specifically good transport properties, stability (both thermal and water/air stability), and tunability. Polyfluorene-based polymers with lower band gap energies have been synthesized for energy conversion applications in attempts to harvest more light at higher wavelengths, i.e., beyond the visible part of the sun's spectrum. Promising results have been reported for solar cells based on various kinds of polyfluorene derivatives (see Refs. 4–7 and references therein).

In this letter, efficient, reproducible bulk heterojunction solar cells have been made by spin casting a chlorobenzene solution of poly[9,9-didecafluorene-alt-(bis-thienylene) benzothiadiazole] (PF10TBT) as electron donor and [C60]PCBM as electron acceptor. PCEs were measured under 1000 W/m², simulated AM1.5 illumination from a WXS-300S-50 solar simulator (WACOM Electric Co.). The mismatch factor (0.99) was calculated using a recent spectrum of the simulator lamp, the spectral responses of, respectively, the used filtered Si reference cell (calibrated at Fraunhofer ISE, Freiburg) and the polymer:fullerene cell. A

more detailed description on device fabrication and electrical characterization can be found in Ref. 8.

Figure 1 shows the current-voltage measurement of the best PF10TBT:[C60]PCBM device [PF10TBT M_w = 34.9 kg/mol; polydispersity index (PDI)=3.6] together with the material structure. The open-circuit voltage (V_{oc}) amounted to 999 mV, the short circuit current (J_{sc}) to 7.7 mA/cm², and the fill factor to 54%, resulting in a PCE of 4.2% (estimated error 5% relatively) for a cell area of 0.36 cm² and a layer thickness of 186 nm. This PCE is among the highest reported for polyfluorene:fullerene photovoltaic cells and it is approaching the best polymer:fullerene efficiency of 4.8%.³ Our latest results are slightly higher than the 3.9% (cell area 0.36 cm²) reported previously⁸ for similar devices, where we used a PF10TBT batch with a higher molecular weight (M_w =58.4 kg/mol; PDI=3.3). The batch with

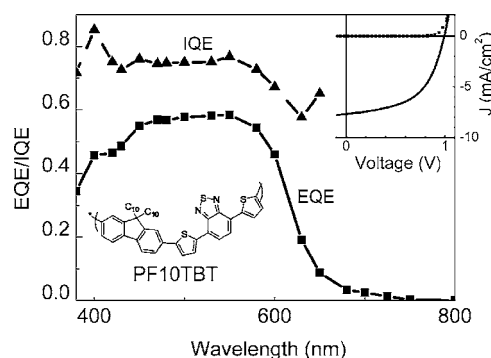


FIG. 1. External quantum efficiency (EQE) measurements of the best PF10TBT:[C60]PCBM photovoltaic cell at short circuit conditions and calculated internal quantum efficiency (IQE). The inset shows the current-voltage measurement of the same device in the dark (squares) and under 1000 W/m² simulated AM1.5 illumination (solid line). Also shown is the molecular structure of PF10TBT.

^{a)}Electronic mail: veenstra@ecn.nl

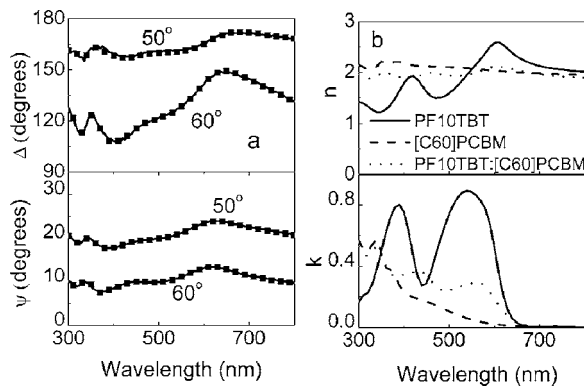


FIG. 2. (a) Ellipsometry parameters Ψ and Δ as a function of wavelength for a 200 nm thick film of PF10TBT:[C60]PCBM on quartz; experimental data (solid line) and the fit of the dispersion model (squares). (b) Refractive index n (top) and extinction coefficient k (bottom) as derived from ellipsometry measurements for PF10TBT (solid line), C60-PCBM (dashed line), and a 1:4 blend of PF10TBT:[C60]PCBM (dotted line).

the high molecular weight was used in the remainder of this letter.

The external quantum efficiency (EQE), measured at short circuit current conditions, of the best device is shown in Fig. 1. As can be seen, in the peak at 550 nm, almost 60% of the incident photons lead to a current in the external circuit. The calculated current based on the overlap between the EQE spectrum and the AM1.5 spectrum is 7.8 mA/cm² which nicely corresponds with the measured AM1.5 current of 7.7 mA/cm². From EQE measurements it cannot be concluded whether the remaining 40% of photons are not absorbed or are absorbed but not contributing to collected charges at the electrodes.

Electrical modeling can provide insight in the working principles of polymer photovoltaic devices^{9–11} and it can be used to determine if there are losses in the charge generation and/or collection. One of the important parameters in these models is the amount of light absorbed in the active layer. Often it is assumed that the absorption is homogeneous or decreases exponentially with increasing film thickness. However, the absorption in these thin film multilayer structures typically exhibits strong interference due to multiple reflection and transmission at the interfaces. In order to address the effect of this interference, optical modeling of these devices must be performed. There are a few reports on the optical modeling of polymer solar cells, showing that optical modeling is a powerful tool in addressing the efficiency of light absorption in the active layer.^{12–14}

Before calculating the light absorption distribution in the Al/LiF/PF10TBT:[C60]PCBM/PEDOT:PSS/ITO/glass stack, ellipsometry measurements were performed to determine the optical constants of the different layers in the cell. The measurements were carried out at the FOM Institute for Atomic and Molecular Physics (Amsterdam, The Netherlands) using a Woollam VASE ellipsometer. All materials were characterized on quartz substrates except for the indium tin oxide (ITO), which was deposited on a glass substrate. Depending on the material, a Cauchy dispersion model, or a combined Lorentz, Tauc-Lorentz oscillator model was used to fit the measured ellipsometry parameters Ψ and Δ .¹⁵ The model fit to the experimental data for the PF10TBT:[C60]PCBM blend material is shown in Fig. 2(a). As can be seen the fit shows excellent agreement with the

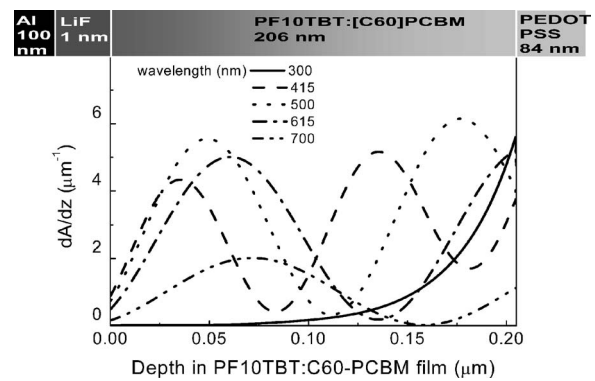


FIG. 3. Absorption distribution within the active layer of a PF10TBT:[C60]PCBM photovoltaic solar cell for various wavelengths of the incident light.

measured data. There are reports in literature on similar materials, showing that the pure polymer material has anisotropic optical constants.^{14,16} However, we did not find any indication for anisotropy in the PF10TBT film. From the model fit, the wavelength dependent refractive index n and extinction coefficient k can be derived and the result is shown in Fig. 2(b) for the 1:4 PF10TBT:[C60]PCBM film as well as for the pure PF10TBT and [C60]PCBM materials. The maximum k of the pure PF10TBT is comparable with the k value obtained for transmission measurements, for which the film thickness was determined using a Dektak surface profiler. This k value is rather high compared to that reported for a similar polymer material.¹⁶ The difference might be due to different stacking in the polymer film resulting from the difference in branching of the polymer side groups. The optical constants of the glass substrate, ITO, PEDOT:PSS, LiF, and Al films were also derived using ellipsometry.

The optical constants were subsequently used to calculate the absorption distribution in the optical software program SCOUT,¹⁷ which uses a transfer matrix formalism.¹⁸ The absorption distribution, $dA(\lambda)/dz$, is shown in Fig. 3 for different wavelengths of the incident photons. The interference patterns resulting from the multiple reflections at the various interfaces are clearly seen. The positions of the interference peaks shift as the wavelength of the incident photons changes. Using these absorption distributions the total number of absorbed photons in the film can be calculated. A wavelength range of 300–800 nm was selected for the incident photons as it coincides with the absorption bands of the PF10TBT and [C60]PCBM. For all these wavelengths the absorption distribution was calculated and integrated over the film thickness to obtain the absorption spectrum $A(\lambda)$ of the film. By taking the convolution of this absorption spectrum with the number of photons in the lamp spectrum ($N_{\text{lamp}}(\lambda)$), the total number of absorbed photons per wavelength was calculated. A final integration over the wavelength range then results in the total number of absorbed photons N .

$$N = \int A(\lambda)N_{\text{lamp}}(\lambda)d\lambda.$$

The lamp spectrum was measured using an Avantes AvaSpec 2048 fiber optic spectrometer. To collect radiation at 180° a CC-UV/VIS cosine corrector is attached to the optic fiber. Before measuring the lamp spectrum an intensity calibration

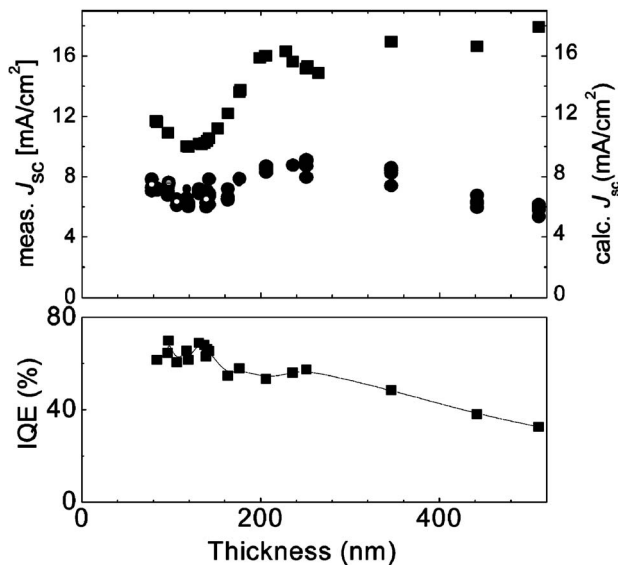


FIG. 4. Top: Measured (circles) and calculated (squares) short circuit current as a function of PF10TBT:[C60]PCBM film thickness. For the calculations, the film thickness of the PEDOT:PSS and blend films of the actual devices was used. Bottom: Total internal quantum efficiency ($J_{\text{measured}}/J_{\text{calc}}$) as a function of layer thickness.

is done using an Avantes HL-2000-CAL tungsten halogen calibration lamp.

Assuming that every absorbed photon results in the collection of charge carriers in the external circuit of the device, i.e., an internal quantum efficiency (IQE) of 100%, the upper limit for the short circuit current density ($J_{sc,max}$) can be calculated. The result is shown in the top part of Fig. 4 as function of the layer thickness. Also shown is the measured short circuit current density (J_{sc}) for a number of PF10TBT:[C60]PCBM photovoltaic cells of various thicknesses. As can be seen, for thin films up to a thickness of 150 nm, the calculated current shows the same trend as the measured current, but with a certain offset. For thicker films, the measured current becomes much lower than the calculated current. This implies that the IQE is decreasing for increasing film thickness. This change in IQE with film thickness is shown in the lower part of Fig. 4 in which the ratio between the measured J_{sc} and calculated $J_{sc,max}$ is plotted. This ratio can be understood as the total IQE, i.e., the IQE averaged over the whole absorption spectrum. From this graph it can be concluded that up to a thickness of roughly 140 nm, 66% of the absorbed photons result in collected charge carriers at the electrodes. At higher film thickness, charge collection starts to become limiting, reducing the IQE substantially. For the best device the IQE spectrum was calculated. This was done by integrating the calculated dA/dz spectrum for different wavelengths, as calculated for this device, over the film thickness. This gives the absorption spectrum in the active layer. Next, the EQE spectrum as shown in Fig. 1 is divided by this calculated absorption spectrum to give the IQE spectrum. The result is shown in Fig. 1. As can be seen, the average IQE is around 75%, which is higher than the IQE calculated for the devices in Fig. 4. This shows

that the better performance of the device is at least partly due to better charge collection.

In summary, a high power conversion efficiency of 4.2% under 1000 W/m² simulated AM1.5 illumination is reported for a PF10TBT:[C60]PCBM photovoltaic cell. It is shown that optical modeling of this type of photovoltaic cells adds to the understanding of the key processes in organic photovoltaic devices. Comparing calculated short circuit currents based on the optical absorption in the device with measured short circuit currents, a distinction can be made between the optical and the electrical contributions in the device. From this it was concluded that for film thicknesses up to 140 nm the IQE is roughly 66%. Further increasing the film thickness does not increase the efficiency due to limitations in charge generation or collection. For this reason it may be interesting to use optical modeling to study how light trapping in the thinner films can be improved. For the 4.2% efficient device, a maximum IQE of about 75% was calculated, indicating improved charge collection.

This work is partly supported by the Dutch Polymer Institute (DPI), project DPI No. 524, and was additionally supported by the Ministry of Economic Affairs of The Netherlands.

¹C. K. Chiang, C. R. Fincher, Jr., Y. W. Park, A. J. Heeger, H. Shirikawa, E. J. Louis, S. C. Gau, and A. G. MacDiarmid, *Phys. Rev. Lett.* **39**, 1098 (1977).

²J.-M. Nunzi, *C. R. Phys.* **3**, 523 (2002).

³M. A. Green, K. Emery, D. L. King, Y. Hishikawa, and W. Warta, *Prog. Photovoltaics* **14**, 455 (2006).

⁴M. Svensson, F. Zhang, S. C. Veenstra, W. J. H. Verhees, J. C. Hummelen, J. M. Kroon, O. Inganäs, and M. R. Andersson, *Adv. Mater. (Weinheim, Ger.)* **15**, 988 (2003).

⁵F. Zhang, K. G. Jespersen, C. Björström, M. Svensson, M. R. Andersson, V. Sundström, K. Magnusson, E. Moons, A. Yartsev, and O. Inganäs, *Adv. Funct. Mater.* **16**, 667 (2006).

⁶R. Pacios, D. D. C. Bradley, J. Nelson, and C. J. Brabec, *Synth. Met.* **137**, 1469 (2003).

⁷Q. Zhou, Q. Hou, L. Zheng, X. Deng, G. Yu, and Y. Cao, *Appl. Phys. Lett.* **84**, 1653 (2004).

⁸D. J. D. Moet, L. H. Slooff, J. M. Kroon, S. S. Chevtchenko, J. Loos, M. M. Koets, J. Sweelssen, and S. C. Veenstra, *Proceedings of the MRS Fall Meeting*, Boston (MRS, Warrendale, PA, 2006), 974E, CC03-09.

⁹L. J. A. Koster, V. D. Mihailetschi, and P. W. M. Blom, *Appl. Phys. Lett.* **88**, 052104 (2006).

¹⁰C. Waldauf, P. Schilinsky, J. Hauch, and C. J. Brabec, *Thin Solid Films* **451-452**, 503 (2004).

¹¹E. A. Katz, D. Faiman, S. M. Tuladhar, J. M. Kroon, M. M. Wienk, T. Fromherz, F. Padinger, C. J. Brabec, and N. S. Sariciftci, *J. Appl. Phys.* **90**, 5343 (2001).

¹²H. Hoppe, N. Arnold, N. S. Sariciftci, and D. Meissner, *Sol. Energy Mater. Sol. Cells* **80**, 105 (2003).

¹³H. Hoppe, N. Arnold, D. Meissner, and N. S. Sariciftci, *Thin Solid Films* **451-452**, 589 (2004).

¹⁴N.-K. Persson, H. Arwin, and O. Inganäs, *J. Appl. Phys.* **97**, 034503 (2005).

¹⁵J. A. Woollam, B. Johs, C. M. Herzinger, J. Hilfiker, R. Synowicki, and C. L. Bungay, *Proc. SPIE* **CR72**, 3 (1999).

¹⁶N.-K. Persson, M. Schubert, and O. Inganäs, *Sol. Energy Mater. Sol. Cells* **83**, 169 (2004).

¹⁷W. Theiss, Hard- and Software, Dr.-Bernhard-Klein-Str. 110, D-52078 Aachen, Germany (www.mtheiss.com).

¹⁸O. S. Heavens, *Optical Properties of Thin Solid Films* (Dover, New York, 1991).